J. Sens. Sens. Syst., 4, 281–288, 2015
www.j-sens-sens-syst.net/4/281/2015/
doi:10.5194/jsss-4-281-2015

JSSS Journal of Sensors and Sensor Systems Open Access

A new low-cost hydrogen sensor build with a thermopile IR detector adapted to measure thermal conductivity

M. Liess

RheinMain University of Applied Sciences, Department of Engineering, Am Brückweg 26, 65428 Rüsselsheim, Germany

Correspondence to: M. Liess (martin.liess@hs-rm.de)

Received: 14 May 2015 – Revised: 16 August 2015 – Accepted: 24 August 2015 – Published: 8 September 2015

Abstract. It is demonstrated how a commercially available MEMS thermopile infrared radiation sensor can be used as thermal conductivity gas detector (TCD). Since a TCD requires a heater while IR-thermopile sensors have no integrated heater, the thermopile itself is used as heater and temperature sensor at the same time. It is exposed to the measured gas environment in its housing. It is shown that, by using a simple driving circuitry, a mass-produced low-cost IR sensor can be used for hydrogen detection in applications such as hydrogen safety and smart gas metering. The sensor was tested to measure hydrogen in nitrogen with concentration of 0–100 % with a noise equivalent concentration of 3.7 ppm.

1 Introduction

In this paper, a new very low-cost hydrogen sensor with high levels of reliability will be introduced. The sensor is based on a thermal conductivity measurement performed with a commercial thermopile IR sensor device. The sensor's performance makes it suitable for applications such as hydrogen measurement in smart gas metering and hydrogen technology safety.

1.1 Motivation

Hydrogen fuel cell systems are of growing interest in the area of sustainable transportation as well as for stationary electric power in remote areas, distributed electric energy generation, in space and other closed environment and auxiliary power systems (Appleby and Foulkes, 1989).

Since a mixture of hydrogen and air is highly explosive in concentrations between 4 and 75 % hydrogen (Kenneth Barbalace, 1995–2015), leakage monitoring is necessary for safety reasons. In particular, the high pressure in hydrogen pressure tanks can lead to significant safety issues (Larminie and Dicks, 2003).

Another use for this kind of sensor is measuring the hydrogen content in natural gas systems. Hydrogen that is produced with electric energy from excess wind and solar energy by electrolysis can be added to existing gas systems (Gahleitner, 2013) up to a content of 5 %. The GERG (European Gas Research Group; Winkler-Goldstein and Rastetter, 2013) sees the potential to add an amount of up to 20 %. In this case, it is necessary to monitor the hydrogen content of the gas at the consumer side to ensure optimization of combustion and smart metering, since the gross heat of combustion of hydrogen (286 $kJ\,mol^{-1}$) and methane (889 $kJ\,mol^{-1}$) are significantly different (Burgess, 2011).

Therefore, reliable and low-cost hydrogen sensors are necessary for leakage monitoring and smart metering of combustible gas.

There are different known sensor principles that allow for hydrogen measurement and detection in a matrix of other gases:

1. The thermal conductivity detector (TCD) or katharometer (Daynes, 1920) detects and distinguishes different gases based on their thermal conductivity and thermal capacity. Since hydrogen has a very high thermal conductivity, the principle of TCD is very suitable for its detection. This principle is treated in more detail in Sect. 1.3.

2. Gas chromatography in combination with TCD, PDD (pulsed discharge ionization detector) BID (barrier discharge ionization detector) as well as mass spectrome-

Published by Copernicus Publications on behalf of the AMA Association for Sensor Technology.

try are also used to determine hydrogen and other gases in complex mixtures. However such methods are rather slow, expensive and more suitable for scientific analysis, rather than safety and consumer purposes.

3. Catalytic sensors or catalytic bead gas sensors measure the combustion heat generated by the chemical reaction of the gas with oxygen on a heated catalytic surface in comparison to a reference surface. Usually catalytic gas sensors are relatively unspecific and react to all combustible gases. However, depending on the catalyst, they might have an enhanced sensitivity to the specific gas concerned (such as hydrogen). A MEMS-catalytic gas sensor has the advantage of miniaturization (Lee et al., 2011). The disadvantage of all catalytic sensors (in addition to their unspecific response) is that they are prone to catalytic poisoning.

4. Palladium-based sensors react to hydrogen due to the high solubility of hydrogen in palladium and subsequent changes to the palladium conductivity, Fermi energy level or work function (Lewis, 1967). Also hydrogen sensors that are based on a Schottky contact between palladium and a semiconductor have been demonstrated (Hudeish and Abdul Aziz, 2006; Song et al., 2005). The disadvantage of all sensors based on Palladium is the fact that this metal is affected by poisoning, for example by sulfur or lead-containing compounds.

   Modern palladium-based sensor designs suitable for low-cost hydrogen measurements exhibit dynamic ranges from 0.025 to 2 % and response times above 1.8 min (Hong et al., 2015), which – for the applications mentioned above – are less suitable than the sensor presented here.

5. Surface acoustic wave (SAW) sensors are based on piezoelectric and, in most cases, additional sensitive materials. In the case of hydrogen detection, the influence of hydrogen on the elasticity of a thin film of WO_3 changes the speed of the surface acoustic waves (Ippolito et al., 2003) and can thus be detected. As with all indirect principles that do not directly react to a physical property of the detected gas, effects of material ageing and poisoning can lead to measurement errors and sensor degeneration.

The sensor presented here is based on a thermal conductivity measurement and a "creative" and new use of a standard, commercially available thermopile IR sensor. Thermopile sensors are mostly used for infrared radiation measurements. They consist of a sensor element that is sealed in a housing and quantifies the energy carried by the radiation to be detected by converting it to heat. In this study, however, an unsealed thermopile sensor is used. The thermopile sensor element not only measures a temperature difference but is also heated by an electric alternating current (AC). At the same time it is cooled by the gas environment which the thermopile is exposed to and measures. Due to the high thermal conductivity of hydrogen, this gas can be detected.

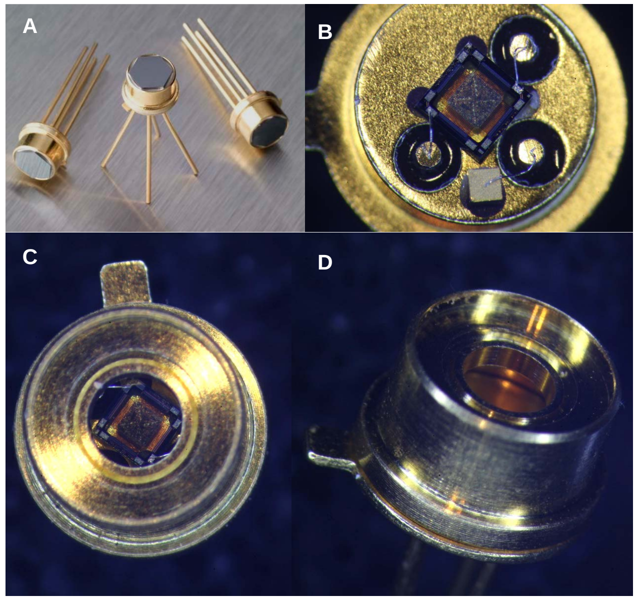

Figure 1. TPS 23B Thermopile sensors. These sensors are a mass product and normally used for IR radiation measurement for example in ear thermometers. **(a)** The image on the upper left (courtesy of Excelitas Technologies GmbH & Co. KG.) shows the sensor as it is used for broadband IR detection in applications such as ear thermometers. **(b)** The image on the upper right shows the interior of the device comprising the sensor element with its thermoelements, the (partially transparent) membrane and the IR-absorber patch. A separate thermistor for ambient temperature compensation is located on the bottom of the device. The parts **(c)** and **(d)** of the figure show sensors that were manufactured without an IR transparent window. Through the "open window", the thermopile sensor element is exposed to the gas environment. In this study they are used as thermal conductivity gas sensors.

1.2 Thermopile IR-radiation sensors

MEMS thermopile sensors (Fig. 1) consist of a thin thermally insulating membrane made of silicon oxide and/or silicon nitride. The membrane is surrounded by a silicon rim/periphery with high thermal conductivity. A large number of thermocouples, forming a thermopile, are placed on the thermally insulating membrane and the silicon periphery in such a way that a temperature difference between membrane and periphery results in a thermoelectric voltage that is multiplied by the number of elements. In the case of the sensor presented, those thermocouples are made of n-doped and p-doped polysilicon.

Thermopile sensors are usually applied in infrared (IR) radiation measurements. In such applications, the IR radiation to be measured heats the so-called "hot contacts" located on the thermally insulting membrane, while the "cold contacts" are on the cold heat-conducting silicon periphery and are not warmed significantly by the incoming IR radiation. Since its thermal behaviour depends on the thermal conductivity of the ambient gas, the IR-thermopile sensor element is usually packaged hermetically with an inert gas filling. IR radiation can enter the packaging through an IR transparent window. In some cases, the packaging is filled with a gas with low thermal conductivity gas. This leads to better isolation of the heated membrane and thus to a higher sensitivity of the device (Graf et al., 2007; Liess, 2012).

Thermopile IR sensors are classically used for contactless temperature measurements through the IR radiation emitted by the object to be measured. They are also used in non-dispersive infrared (NDIR) gas sensors to detect gases through their specific IR absorption lines (Graf et al., 2007). The method presented in this paper is not related to the well-known method of NDIR or any kind of IR detection.

Thermopile sensors are very sensitive to electric currents driven into their output terminals since this leads to resistive heating of the thermocouple structure and thus of the membrane of the sensor element. The resulting thermal gradient generates an error signal. This can be of relevance since, for example, a chopper amplifier (Wu et al., 2013) can capacitively couple alternating currents unintentionally into the sensor. This AC error itself is filtered by the low-pass properties of the amplifier and signal conditioning electronics and is therefore of no relevance. However it leads to an ohmic heating effect within the thermopile, which in turn generates a DC error that has the same properties as the measured IR signal and cannot be filtered.

Thermopile IR sensors are thus cross-sensitive to input average currents and to a leakage of the filling gas. Exactly these properties are used in this study to build a gas sensor.

1.3 Stability of the presented sensor

The modified CMOS production process of thermopile sensors involves high temperatures and harsh processes such as potassium hydroxide etching and photoresist removal. Thus the sensor element can be expected to be very stable against thermal and chemical damage caused by environmental influences.

In automotive applications (Liess et al., 2004), including racing sports, the sensor design has demonstrated a quasi-unlimited lifetime over the years and high mechanical robustness as an IR-radiation sensor.

The physical measurement principle is based on heat conduction and does not involve the chemical interaction of the measured environment with any part of the sensor. The sensor surface is passivated by a layer of silicon nitride so that the sensing elements are not exposed to any materials that could give rise to poisoning or a change to the doping of the polysilicon. Furthermore, the films are heavily doped with doses of 5×10^{15}–15×10^{15} atoms cm^{-3} and dopant diffusion is expected to be low at operation temperatures, which are significantly below the diffusion temperature of around 1000 °C. Therefore, sensitivity changes or any kind of poisoning of the sensitive parts of the device cannot be expected due to the chemical effects of the measured environment.

Table 1. Examples of the thermal conductivity of different gases. Data from Young and Sears (1992).

Gas	Thermal conductivity at 20 °C [$W\,(m \cdot K)^{-1}$]
Nitrogen	0.0234
Oxygen	0.0238
Hydrogen	0.172
Air (at 0 °C)	0.024
Helium	0.138

1.4 Thermal conductivity gas sensors

Commercially available TCDs are based on four identical platinum resistors that are arranged in a bridge configuration and are electrically heated. The voltage drop on each platinum resistor indicates its resistance and is thus a measure of its temperature. Since two resistors are exposed to the gas to be measured and the two other resistors are exposed to a reference gas, differences in the heat conductivity between the measured gas and reference gas lead to a bridge voltage. As can be seen in Table 1, hydrogen has a 7 times higher thermal conductivity than air. Hydrogen's high thermal conductivity is paralleled only by helium, which is not present in the typical environment where hydrogen needs to be detected.

De Graaf and Wolffenbuttel (2012) developed a micromachined thermal conductivity gas sensor, based on a thermopile for temperature measurement and a dedicated heater for heating the hot contacts of the thermopile. The sensor has, in addition, a dedicated sample chamber, made by a surface micromachining processes. To obtain a stable signal, heat modulation and a lock-in technique is used.

1.5 Operating principle of the sensor presented here

The sensor used in this work (Fig. 1) is a commercially available thermopile IR sensor that is available for applications such as ear thermometers on the mass market. The sensor itself has two output contacts. Usually they output a DC voltage that is proportional to the IR radiation, which the sensor element receives. However, in this application, the same two pins are used to input an AC heating voltage into the device and to output, at the same time, the DC signal voltage, which measures the hydrogen concentration. Also the thermopile structure itself is now used for two purposes: its resistive properties are used for heating (by an AC voltage) and its thermoelectric properties are used for measuring a temperature difference (by a DC voltage). In order to enable this mode of operation the sensor is connected through a high-pass circuit to the AC heating supply and gives out its DC signal through a low-pass circuit. The gas to be measured is simply supplied to the surface of the sensor and contained by the standard sensor housing (Fig. 2).

2 Experimental section

2.1 A MEMS thermopile used as a thermal gas sensor

A thermopile sensor can be used as a hydrogen sensor because of

- the high thermal conductivity of hydrogen,
- the cross-sensitivity of thermopile sensors toward their gas environment,
- the error sensitivity toward AC input currents into the sensor's output terminals.

For gas sensor operation, commercially available thermopile IR-sensor devices have been used that are manufactured without an IR window (Fig. 1) so that the sensor element can be directly exposed to the gas environment. The membrane of the sensor element is heated by an AC that is applied to the input terminals of the thermopile sensor (Liess, 2014). The thermopile's DC output voltage is then measured.

2.2 Electrical setup

An Agilent Technologies Function/Arbitrary-Waveform generator 80 MHz 33250A frequency generator was used to supply the AC driving voltage to the sensor. Using a capacitor, the frequency generator is decoupled from DC voltages generated in the circuit. The AC voltage is applied to a thermopile sensor. The DC voltage generated by the thermopile is filtered by a low-pass filter comprising a resistor and a capacitor and measured by a Fluke 77 IV digital multimeter. The electrical setup is shown in Fig. 2. Measurement curves over extended periods of time were recorded using the capabilities of a modified gas analyser manufactured by Emerson Process Management GmbH & Co. OHG.

2.3 Driving a thermopile with AC voltage

The heat P_{heat} generated inside the sensor element by an AC voltage U_{AC} applied to the output terminals of the thermopile sensor follows the equation

$$P_{\mathrm{heat}} = \frac{U_{\mathrm{AC}}^2}{R_{\mathrm{sensor}}}. \quad (1)$$

One can assume that the thermal contact between the periphery and the ambient is so good that the temperatures of the periphery and the ambient environment are identical. They are equal to T_{amb}. Since a fraction A of the heat P_{heat} is generated on the membrane, its temperature T_{mem} depends

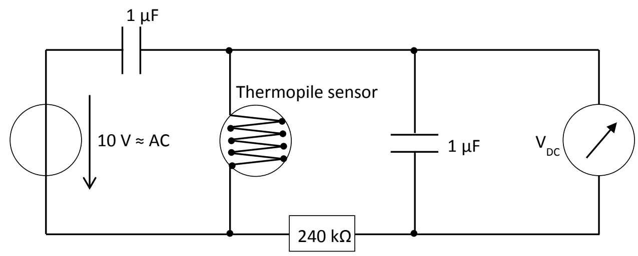

Figure 2. Electrical circuit for driving the thermopile as gas sensor. Inner resistance of the sensor is 120 kΩ.

on the thermal contact between the membrane and the periphery λ_{mem} and the gas λ_{gas} as

$$T_{\mathrm{mem}} = \frac{A \cdot P_{\mathrm{heat}}}{\lambda_{\mathrm{mem}} + \lambda_{\mathrm{gas}}} + T_{\mathrm{amb}}. \quad (2)$$

Here, the thermal contact λ is defined as (thermal conductivity) · (contact area)/(length of the contact). The generated thermopile voltage U is proportional to the temperature difference ΔT between the membrane and the periphery

$$U_{\mathrm{DC}} \propto \Delta T = \left(T_{\mathrm{mem}} - T_{\mathrm{per}}\right) \approx \frac{A \cdot P_{\mathrm{heat}}}{\lambda_{\mathrm{mem}} + \lambda_{\mathrm{gas}}}. \quad (3)$$

Thus,

$$U_{\mathrm{DC}} \propto \frac{U_{\mathrm{AC}}^2}{\lambda_{\mathrm{mem}} + \lambda_{\mathrm{gas}}}. \quad (4)$$

2.4 Mechanical setup

Two thermopile sensors (Excelitas Technologies, Wiesbaden, Germany) type TPS 23B without an IR window (Fig. 1) were connected to the electrical setup. They were exposed to nitrogen, hydrogen, or any mixture of these gases at different temperatures using a climate chamber. The gas mixtures were produced by a DIGAMIX KM301 Wösthoff gas mixing pump and measured with a variable area flow meter. Different flow rates of nitrogen were generated using a needle valve and a variable area flow meter. Figure 3 shows the mechanical setup. The sensors are exposed to the gas flow using T-junctions and are sealed with O-rings. By mounting the sensor in the slipstream (Fig. 3) about 1 cm off of the main stream, the sensor is exposed to the gas but not to its direct flow; 6 mm diameter Swagelok stainless steel tubing and materials were used.

3 Results and discussion

3.1 Response of the thermopile sensor to an AC voltage

In the first experiments, the functionality of the electronic setup was verified. Figure 4 demonstrates that the idea of applying an AC voltage to the sensor through a high-pass filter,

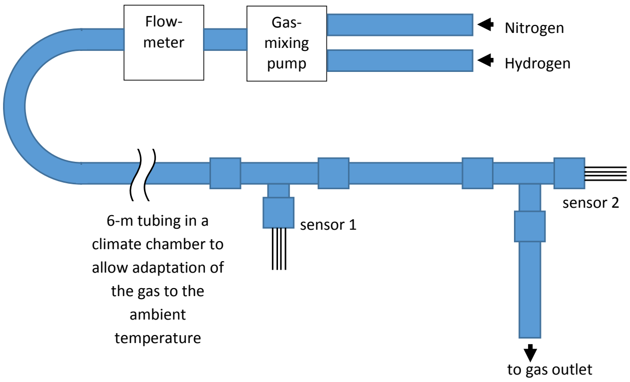

Figure 3. Drawing of the gas tubing with the thermopiles. The sensors are fitted in T-junctions within stainless steel tubing inside a climate chamber.

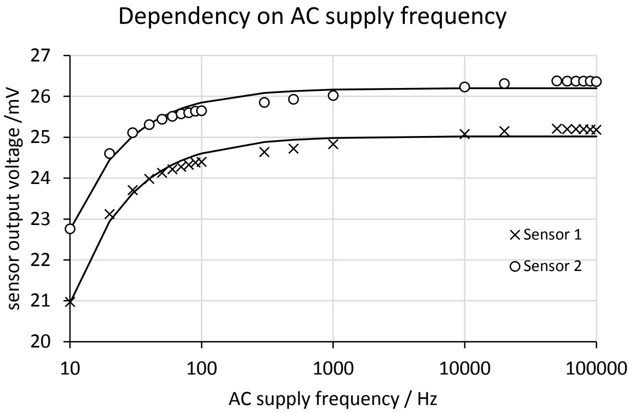

Figure 4. Frequency dependence of the sensor signal in the ambient environment. The lines represent the behaviour of first-order high-pass filters with cut-off frequencies of 1.9 and 2.4 Hz.

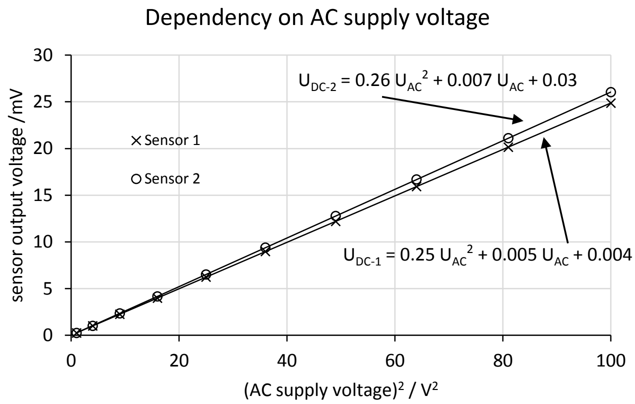

Figure 5. AC supply voltage dependence of the sensor signal in a room environment. The lines represent polynomial fits of the third order with no constraints. It can be seen that, within the range of supply voltages, the quadratic term is 370–500 times greater than any other term, indicating that the measured signal represents a DC thermovoltage generated by ohmic heating of alternating currents through the thermopile. The power applied to the sensor calculates as $P = U^2/R$. Since $R = 120\,\mathrm{k\Omega}$, the maximum power is 0.83 mW.

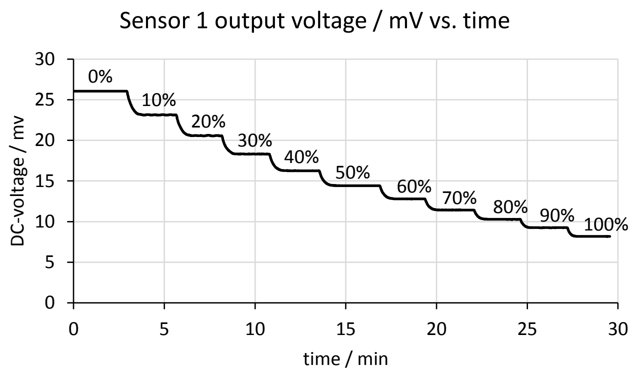

Figure 6. Measurements of the sensor 1 signal with different H_2 concentrations. The measurements were performed at 5 °C in a climate-controlled room. If not indicated differently, all measurements were performed at flow rates of 0.5 L min^{-1}.

constituted by a capacitor and the sensor's inner resistance, and measuring the output DC voltage through a low-pass filter works well. It can be seen that the AC input to the thermopile sensor generates a DC output.

Figure 5 shows a simple quadratic dependence between input AC and output DC voltage with practically no zeroth- and first-order terms, indicating that the input AC voltage is converted to ohmic heat, which is – within a reasonable approximation – the only source of a temperature gradient that leads to the signal from the thermopile sensor. A significant first-order term would have indicated a prominent Peltier effect. This was not observed, which is in agreement with the fact that, firstly, the quadratic effect of ohmic heating dominates over Peltier heat transport at high driving voltages and, secondly, AC voltage was used for driving the sensor. A significant zeroth-order term (offset) would have indicated a strong external heat source or a high temperature difference between the gas and the sensor. This was not observed since the sensor was operated in equilibrium with the measured gas.

3.2 Response of the DC sensor output voltage to the H_2 concentration

To test the effect of the gas environment, the sensors were exposed to mixtures of hydrogen in nitrogen in steps of 10 or 0.5 % of a few minutes in duration, while the sensor's output voltage was measured (Figs. 6 and 7). It can be seen that, despite the simple measurement setup, the signal can easily be distinguished from the noise.

Due to the transfer of inertia and energy between the different atoms, the heat conductivity of mixtures between hydrogen and nitrogen is not a simple linear function of

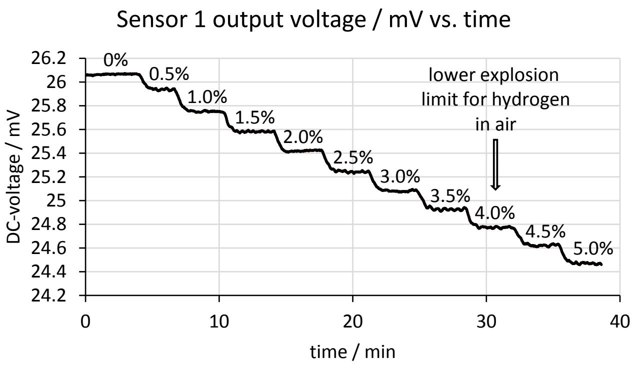

Figure 7. Measurements of the sensor 1 signal with different low H_2 concentrations. The measurements were performed at 5 °C in a climate-controlled room. The lower detection limit of 4 % hydrogen can easily be distinguished by a sensor output voltage drop of 4.8 % as compared to the output voltage in the air.

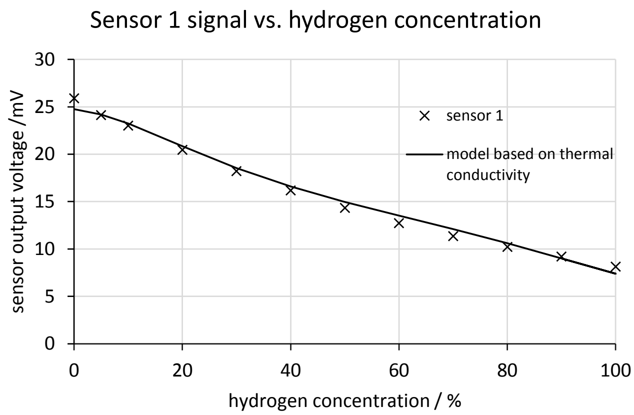

Figure 8. Comparison of the measured data with sensor 1 to a model based on Eq. (1) and literature heat conductivity values of mixtures between hydrogen and nitrogen (Mason and Saxena, 1958).

their concentration. Experimental heat conductivity data of mixtures between hydrogen and nitrogen at 0 °C (Mason and Saxena, 1958) were used in Eq. (1) together with the heat conductivity of the membrane that was fitted using the Levenberg–Marquardt algorithm to match the sensor signal (Fig. 8). A good agreement was obtained. The heat conductivity of a hydrogen environment can be calculated as 4.38 times higher than the heat conductivity of the membrane, while the heat conductivity of a nitrogen environment is lower than the heat conductivity of the membrane by a factor of 0.61.

3.3 Basic sensor specifications

The sensitivity (Fig. 9), the dynamic response ($\tau = 2.5$ s) and the measurement's rms noise level (3.7 µV) were calculated from the data of the output voltage versus changing H_2 concentration (Fig. 6). It can be seen that the dynamic response

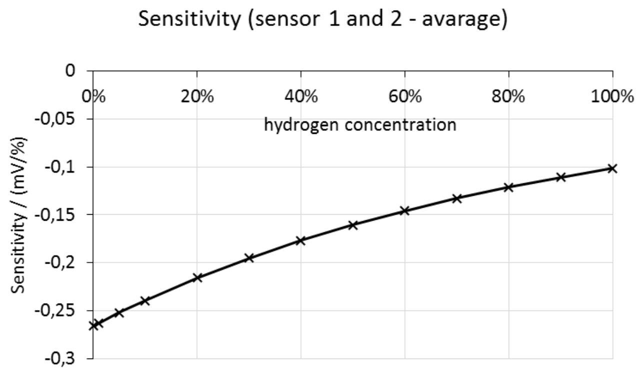

Figure 9. Sensitivity at different hydrogen concentrations.

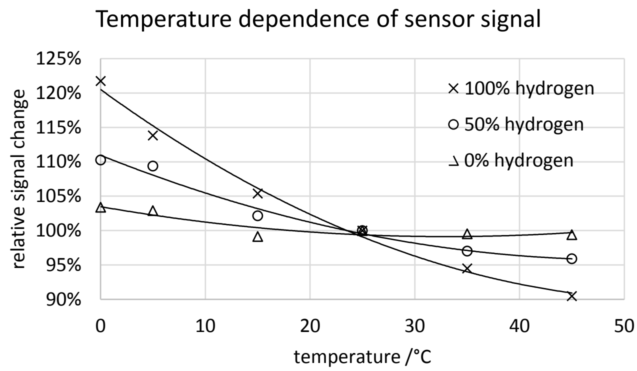

Figure 10. Temperature dependence of the sensor output voltage at different hydrogen concentrations.

is significantly smaller than the thermal response (15 ms) of the device as indicated by the sensor's manufacturer. This indicates that the dynamic response is limited by the diffusion of the gas to the sensor that is mounted in the slipstream of the dead end of the T-junction (Fig. 3) and not by the sensor properties themselves.

The noise level of the sensor can be calculated from the thermal or Johnson noise due to its inner resistance (120 kΩ). It can be seen that the noise level of the measurement is not due to the sensor itself but due to the driving and signal recording electronic circuitry. The basic specifications of the sensor and the measurement are compiled in Table 2.

3.4 Temperature and flow rate cross-sensitivity measurements

Even though the relative temperature dependence of the heat conductivity of hydrogen and air (Davies, 2006) remains similar in the relevant temperature range, the temperature dependence of the sensor reading increases with larger hydrogen concentrations (Fig. 10). This can be attributed to the fact that, with rising hydrogen concentration and thus rising thermal conductivity of the gas environment, its temperature-dependent contribution rises. In contrast, the thermal conduc-

Table 2. Compilation of basic sensor and measurement specifications.

	Value/unit	Comment
Sensitivity	-27 to $-10\,\mathrm{mV}\,\%^{-1}$	At concentrations of 0–100 % hydrogen (compare Fig. 9)
Intrinsic thermal time constant	15 ms	From manufacturer's data sheet
Time constant limited by gas diffusion	2.5 s	As observed in the measurements shown in Fig. 6
Sensor chip inner resistance	120 kΩ	From manufacturer's data sheet
Rms noise level of the measurement	3.7 µV	Calculated during the first 3 min of the measurement shown in Fig. 6
Rms noise level of the sensor during 3 min of measurement with measurement rate of 1.75 Hz	0.06 µV	Calculated from the thermal or Johnson noise at 20 °C for a 120 kΩ sensor
Noise equivalent concentration of the measurement	1.4–3.7 ppm (H_2)	Calculated from measured rms noise and the measured sensitivity at 0–100 % hydrogen concentration
Cross-sensitivity towards the flow velocity	max. 15 ppm (H_2)/($\mathrm{m\,s^{-1}}$)	Calculated from the data of Fig. 11 and the device's minimum sensitivity at 100 % %H_2 concentration (Fig. 9)
Cross-sensitivity towards the temperature	-9 to -30 ppm (H_2) $\mathrm{K^{-1}}$	Calculated from the data of Fig. 10 and the sensitivity shown in Fig. 9 for 0–100 % %H_2

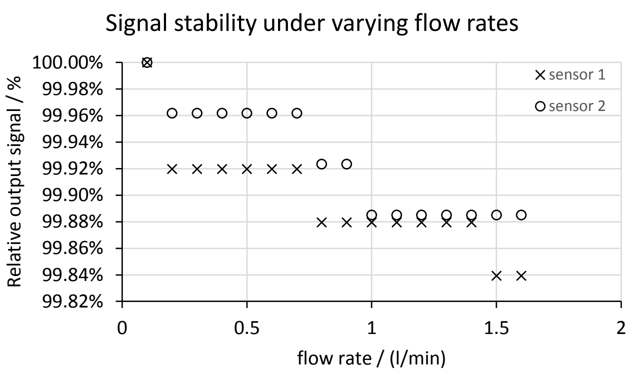

Figure 11. Flow rate dependence of the sensor output voltage for flow velocities up to $1\,\mathrm{m\,s^{-1}}$. At the flow rate of $1\,\mathrm{L\,min^{-1}}$ the flow velocity is $0.59\,\mathrm{m\,s^{-1}}$.

tivity of the sensor membrane is constant with temperature and dominates the behaviour of the sensor at low hydrogen concentrations. As with other hydrogen sensors, such as classical TCDs, the temperature of the sensor must be stabilized to allow for precise measurements, or the effect of the ambient temperature must be compensated after the measurement. Since a thermistor temperature probe is part of most thermopile sensor devices, temperature measurement and compensation is possible without any additional effort.

Within the commercial temperature range from 0 to 85 °C, the maximum measurement error caused by temperature effects can be calculated. It is smaller than 0.26 % (H_2) within the full measurement range, 0.08 % (H_2) for hydrogen concentrations of below 5 % and smaller than 0.1 % (H_2) for hydrogen concentrations of less than 20 % (Fig. 10). Therefore, for hydrogen safety and smart metering, no temperature compensation of the sensor signal is necessary.

Since for hydrogen concentrations up to 20 % the maximum measurement error caused by gas flow velocities of up to $1\,\mathrm{m\,s^{-1}}$ is smaller than 7.3 ppm (H_2) (Fig. 11), no flow rate compensation must be applied for use of these sensors in hydrogen safety and smart metering.

4 Conclusions and outlook

It was demonstrated that a thermopile sensor with suitable simple driving circuitry, which is exposed to a mixture of hydrogen and a heavier gas (for example nitrogen or air), can be used as a low-cost thermal hydrogen gas sensor. It behaves according to the theoretical expectations.

The sensor is suitable for applications such as hydrogen technology safety and smart gas metering without compensation of ambient temperature and gas flow velocity. If mounted in the slipstream of an approximately 1 cm long dead-end tube, the sensor exhibits basically no cross-sensitivity toward the flow rate and reacts sufficiently fast (2.5 s).

The idea of using a thermopile as a heater and temperature difference sensor at the same time can also be applied in other sensor principles. This allows for simplification of the design or even for use of the same MEMS sensor element for different purposes (like IR sensing, gas sensing or flow sensing) depending on the driving circuitry, housing and exposure to the measured magnitudes.

It was also demonstrated how sensor shortcomings (of a MEMS thermopile IR-radiation sensor) can be used to create a new sensor for a different purpose (when the sensor is used as a gas sensor). Thus also here Edward W Ng's famous quote "One man's noise is another man's signal" (Blackslee, 1990) applies well.

Acknowledgements. I thank M.-K. Winter and H. Krause of Emerson Process Management in Hasselroth for their support in facilitating the measurements and for financial support. I also express my gratitude to the team of Excelitas Technologies GmbH & Co. KG, who manufactured the custom thermopile sensor devices without IR windows for these experiments.

Edited by: S. Schmid
Reviewed by: two anonymous referees

References

Appleby, A. J. and Foulkes, F. R.: Fuel cell handbook, Van Nostrand Reinhold, New York, USA, XXVI, 762 pp., 1989.

Blackslee, S.: Lost on Earth: Wealth of Data Found in Space: "In science, one man's noise is another man's signal", New York Times, available at: http://www.nytimes.com/1990/03/20/science/lost-on-earth-wealth-of-data-found-in-space.html (last access: 12 May 2015), 1990.

Burgess, D. R.: Thermochemical Data, in: NIST Chemistry WebBook: NIST Standard Reference Database Number 69, edited by: Linstrom, P. J. and Mallard, W. G., Gaithersburg, MD, USA, available at: http://webbook.nist.gov (last access: 30 April 2015), 2011.

Davies, T. W.: Thermal Conductivity Values, in: A-to-Z Guide to Thermodynamics, Heat and Mass Transfer, and Fluids Engineering, Begellhouse, Redding, Connecticut, USA, 2006.

Daynes, H. A.: The Theory of the Katharometer (with an Introductury Note by G. A. Shakespear), Proc. Roy. Soc. London A, 273–286, 1920.

de Graaf, G. and Wolffenbuttel, R. F.: Surface-micromachined thermal conductivity detectors for gas sensing, in: 2012 IEEE International Instrumentation and Measurement Technology Conference (I2MTC), 13–16 May 2012, Graz, Austria, 1861–1864, 2012.

Gahleitner, G.: Hydrogen from renewable electricity: An international review of power-to-gas pilot plants for stationary applications, Int. J. Hydrogen Energ., 38, 2039–2061, 2013.

Graf, A., Arndt, M., Sauer, M., and Gerlach, G.: Review of micromachined thermopiles for infrared detection, Meas. Sci. Technol., 18, R59–R75, 2007.

Hong, J., Lee, S., Seo, J., Pyo, S., Kim, J., and Lee, T.: A highly sensitive hydrogen sensor with gas selectivity using a PMMA membrane-coated Pd nanoparticle/single-layer graphene hybrid, ACS Appl. Mater. Interfaces, 7, 3554–3561, doi:10.1021/am5073645, 2015.

Hudeish, A. Y. and Abdul Aziz, A.: A hydrogen sensitive Pd/GaN schottky diode sensor, J. Phys. Sci., 17, 161–167, 2006.

Ippolito, S. J., Kandasamy, S., Kalantar-Zadeh, K., Trinchi, A., and Wlodarski, W.: A Layered Surface Acoustic Wave ZnO/$LiTaO_3$ Structure with a WO_3 Selective Layer for Hydrogen Sensing, Sen. Lett., 1, 33–36, doi:10.1166/sl.2003.007, 2003.

Kenneth Barbalace: Periodic Table of Elements – Hydrogen – H, EnvironmentalChemistry.com, available at:http://EnvironmentalChemistry.com/yogi/periodic/H.html (last access: 31 August 2015), 1995–2015.

Larminie, J. and Dicks, A.: Fuel cell systems explained, SAE International and John Wiley & Sons, Ltd., 428 pp., 2003.

Lee, E.-B., Hwang, I.-S., Cha, J.-H., Lee, H.-J., Lee, W.-B., Pak, J. J., Lee, J.-H., and Ju, B.-K.: Micromachined catalytic combustible hydrogen gas sensor, Sensor. Actuat. B-Chem., 153, 392–397, doi:10.1016/j.snb.2010.11.004, 2011.

Lewis, F. A.: The Palladium Hydrogen System, Academic Press, London, UK, New York, USA, 1967.

Liess, M.: 14 Fotoelektrische Sensoren, in: Sensoren in Wissenschaft und Technik: Funktionsweise und Einsatzgebiete, edited by: Hering, E., Vieweg+Teubner Verlag, Wiesbaden, Germany, 609–628, 2012.

Liess, M.: A new principle for low-cost hydrogen sensors for fuel cell technology safety, in: 4th International Conference on Mathmatics and Natural Sciences (ICMNS 2012): Science for Health, Food and Sustainable Energy, Bandung, Indonesia, 8–9 November 2012, AIP Conference Proceedings, AIP Publishing LLC, 522–525, 2014.

Liess, M., Hausner, M., Schilz, J., Lauck, G., Karagoezoglu, H., and Ernst, H.: Temperature radiation sensors for automotive climate control, in: IEEE Sensors, 2004, Vienna, Austria, 24–27 October 2004, 5–7, 2004.

Mason, E. A. and Saxena, S. C.: Approximate Formula for the Thermal Conductivity of Gas Mixtures, Phys. Fluids, 1, 361, doi:10.1063/1.1724352, 1958.

Song, J., Lu, W., Flynn, J. S., and Brandes, G. R.: AlGaN/GaN Schottky diode hydrogen sensor performance at high temperatures with different catalytic metals, Solid State Electron., 49, 1330–1334, doi:10.1016/j.sse.2005.05.013, 2005.

Winkler-Goldstein, R. and Rastetter, A.: Power to Gas: The Final Breakthrough for the Hydrogen Economy?, Green, 3, 69–78, doi:10.1515/green-2013-0001, 2013.

Wu, R., Huijsing, J. H., and Makinwa, K. A. A.: Precision Instrumentation Amplifiers and Read-Out Integrated Circuits, Springer New York, New York, USA, Online-Ressource, 196 pp., 2013.

Young, H. D. and Sears, F. W.: University physics, 8th ed., Addison-Wesley Pub. Co., Boston, USA, xx, 1132 pp., 1992.